



## Polysaccharides from fermented coix seed modulates circulating nitrogen and immune function by altering gut microbiota

Hui Wang<sup>a,1</sup>, Hongmei Yin<sup>a,b,1</sup>, Yadong Zhong<sup>a</sup>, Jielun Hu<sup>a</sup>, Shengkun Xia<sup>a</sup>, Zixuan Wang<sup>a</sup>, Shaoping Nie<sup>a</sup>, Mingyong Xie<sup>a,\*</sup>

<sup>a</sup> State Key Laboratory of Food Science and Technology, China-Canada Joint Laboratory of Food Science and Technology (Nanchang), Key Laboratory of Bioactive Polysaccharides of Jiangxi Province, Nanchang University, 235 Nanjing East Road, Nanchang, Jiangxi, 330047, China

<sup>b</sup> School of Health, Jiangxi Normal University, 99 Ziyang Avenue, Nanchang, Jiangxi, 330022, China

### ARTICLE INFO

#### Keywords:

Coix seed  
Polysaccharides  
Circulating nitrogen  
Gut microbiota  
Immune homeostasis

### ABSTRACT

*Coix lachryma-jobi* L. seed is an important food item in Asia with culinary and medicinal values. The effects of non-fermented coix seed (NFC), fermented coix seed with *Lactobacillus plantarum* NCU137 (FC) and polysaccharides from NFC, FC (FCP) on mice circulating nitrogen and immune disorder induced by high relative humidity (RH, 90 ± 2%) exposure were compared. All the treatments reduced circulating nitrogen (BUN and ammonia) might via increasing excretion of fecal nitrogen induced by altering gut microbiota. In comparison, FC and FCP restored erythrocyte morphology by promoting erythrocyte Na<sup>+</sup>/K<sup>+</sup> ATPase activity more effectively, and immune function was modulated by reducing plasma IgM and IFN-γ levels, up-regulating IL-4 and IL-6 levels. Herein, these results indicated that FCP, as the main active ingredient in FC, modulated circulating nitrogen through altering gut microbiota, and restored immune homeostasis by regulating Th1/Th2 cytokines in mice receiving high RH exposure.

### 1. Introduction

Intestinal luminal nitrogen metabolism played a crucial role in gut microbiota and consequences of host (Davila et al., 2013). Urea has long been considered as an inert molecule. However, it was reported to induce disruption of the intestinal barrier by decreasing expression of the tight junction proteins occludin, claudin-1 and ZO-1 (Vanholder et al., 2018). Nitrogen metabolism include short-chain fatty acids and tryptophan metabolites were reported to influence immune maturation, immune homeostasis, host energy metabolism and maintenance of mucosal integrity in inflammatory bowel disease (Lavelle and Sokol, 2020). An increase in fecal amino acids content was found to be positively correlated with Crohn's disease activity, with the mechanism that gut microbiota dysbiosis promoted bacterial urease-mediated change in nitrogen flux (Ni et al., 2017). A similar mechanism was also found in multiple myeloma, which an increase in the relative abundance of nitrogen-recycling bacteria accelerated the disease progression via degradation of urea, *de novo* synthesis of glutamine and then absorption by the host (Jian et al., 2020). The similar studies reported that the gut

microbiota-osteoporosis association might be explained by altered amino acid metabolism of feces and serum in a large cohort (Ling et al., 2020). Beside, ammonia is considered as a direct toxic effect on colonic cells, of which life span was shortened (Lin & Visek, 1991). To figure out circulating ammonia or urea by the microbiome contribute to nitrogen availability for tumors or immune cells might help us to understand the requirements and metabolic constraints in these cell types and may ultimately aid in identifying areas of intervention for cancer therapy (Kurmi and Haigis, 2020).

Plant polysaccharides are a major energy source for gut bacteria, microbial fermentation products, in turn, provide energy and nutrients to the host (Flint et al., 2008; Fang et al., 2021). To our knowledge, polysaccharides have important biological activities and functions via regulating intestinal flora disorders and promoting microbial metabolism, including tryptophan metabolism (Yang et al., 2021; Song et al., 2021; Lin et al., 2021), short-chain fatty acids metabolism (Yu et al., 2022), amino acids and nucleic acid metabolism (Chen et al., 2020). *Coix lachryma-jobi* L. seed polysaccharides have been reported to have anti-oxidative, gut microbiota modification, immunological

\* Corresponding author.

E-mail address: [myxie@ncu.edu.cn](mailto:myxie@ncu.edu.cn) (M. Xie).

<sup>1</sup> Authors contributed equally to this work.

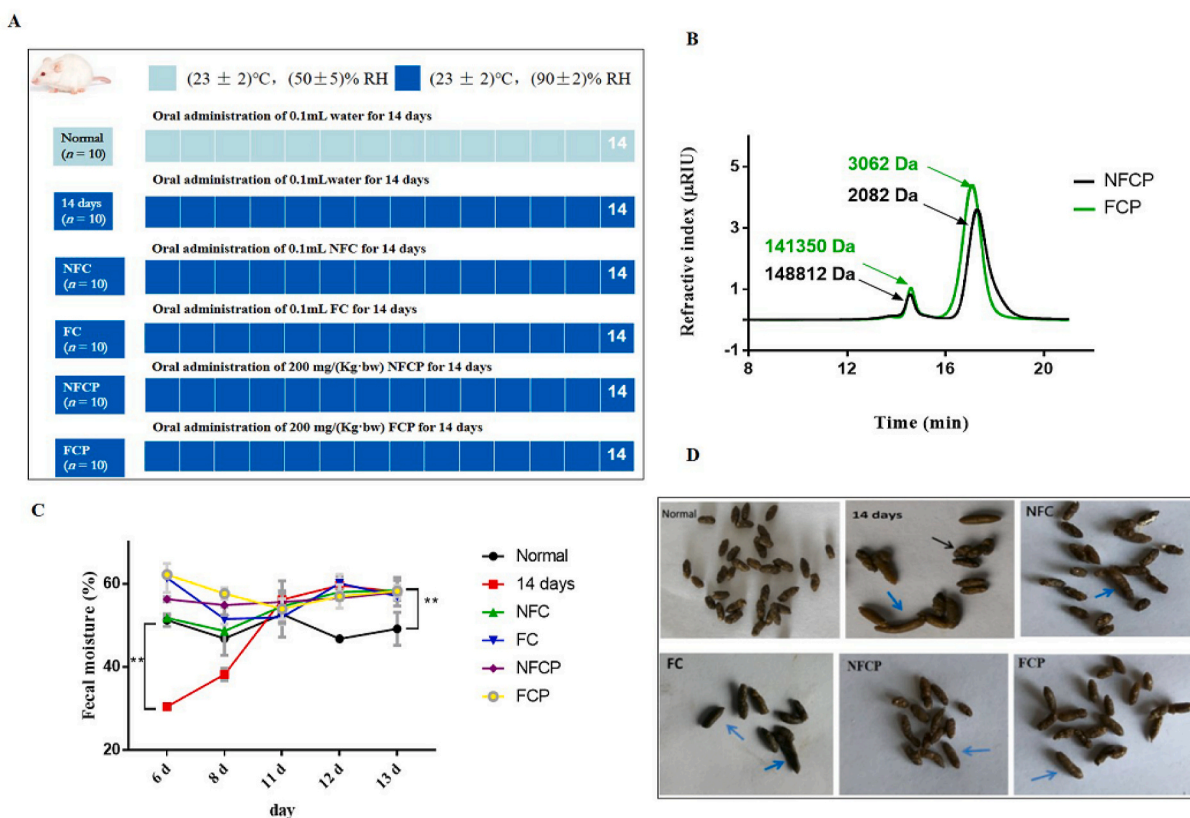


**Fig. 1.** The animal experiment design (A), molecular weight distribution of NFCP and FCP (B), the fecal moisture (C) and appearances (D) of mice. The black arrows that the feces are dry and rough, while the blue arrows indicate the feces contain high moisture content. (For interpretation of the references to colour in this figure legend, the reader is referred to the Web version of this article.)

**Table 1**

The chemical composition of NFCP and FCP.

Samples	Yield (%)	Neutral sugar (%)	Uronic acid (%)	Protein (%)	Monosaccharide composition (%)
					Glc
NFCP	179.80 ± 8.00	81.58 ± 3.07	10.42 ± 0.19	4.07 ± 0.03	68.61 ± 1.83
FCP	359.27 ± 79.75*	81.66 ± 0.07	9.05 ± 0.49*	1.37 ± 0.08*	72.91 ± 2.71

Data were expressed as M ± SD, n = 3.

modulation, hypolipidemic, hypoglycemic and anti-cancer activities (Yin et al., 2018).

Growing evidence reported that lactic acid bacteria fermented foods had the potential of decreasing insulin resistance, improving gastrointestinal health and enhancing gut barrier function (De Filippis, Pasolli and Ercolini, 2020). In our previous study, we found that the nutritional, sensory and stability properties of coix seed were improved by *Lactobacillus plantarum* NCU137 fermentation, due to the production of new substances, including butyric acid and soluble dietary fiber (Yin et al., 2020). Moreover, we demonstrated that colonic urea-nitrogen metabolism and gut microbiota are disrupted in mice exposing to high relative humidity (RH, 90 ± 2%), which might be induced by the increased circulating nitrogen (Yin et al., 2022). The present study was aimed to compare the regulatory effects of non-fermented, fermented coix seed and polysaccharides on circulating nitrogen and immune function of mice exposed to high RH. Then, the composition of gut microbiota was analyzed to explore the possible related mechanisms. It might provide new insights into developing coix seed-based effective and safe intervening strategies for the prevention of immune function and circulating nitrogen disordered.

## 2. Materials and methods

### 2.1. Materials

Coix seed was obtained from the local market, which is origin from Chifeng, Inner Mongolia. *Lactobacillus plantarum* NCU137 powder was preserved at -20 °C in our laboratory. The α-amylase (120,000 U/g) and amyloglucosidase (100,000 U/g) were purchased from Novozymes (Copenhagen, Denmark). Papin (650,000 U/g) was provided by Pangbo Enzyme (Guangxi, China). Antidiuretic hormone (ADH) ELISA kit was obtained from Enzyme-linked Biotechnology (Shanghai, China). Na<sup>+</sup>/K<sup>+</sup> ATPase activity, IL-6, IL-4, IL-10 and IFN-γ ELISA kits were purchased from SenBeiJia (Jiangsu, China). The blood urea nitrogen (BUN) and ammonia kits were provided by Jiancheng (Jiangsu, China). IgA, IgM and IgG ELISA kits were obtained from USCN (Wuhan, China). All other drugs and reagents used were of analytical grade (Sigma, USA).

### 2.2. Preparation of non-fermented and fermented coix seed

The non-fermented coix seed (NFC) and fermented coix seed with *L. plantarum* NCU137 (FC) were prepared according to the method of our pervious study (Yin et al., 2020).

### 2.3. Preparation of polysaccharides

The fermented and non-fermented coix seed were extracted with ultrapure water (1:5, W/V) at 95 °C for 1 h for twice. After centrifugation (827 g for 15 min), the supernatant was hydrolyzed by α-amylase (95 °C for 2 h), amyloglucosidase (60 °C for 30 min), and papin (60 °C for 1 h) to successively remove starches and proteins. During the whole process, the enzymes were inactivated at 100 °C for 10 min after each of these enzymatic processes. After that, centrifugated (827 g for 15 min), the

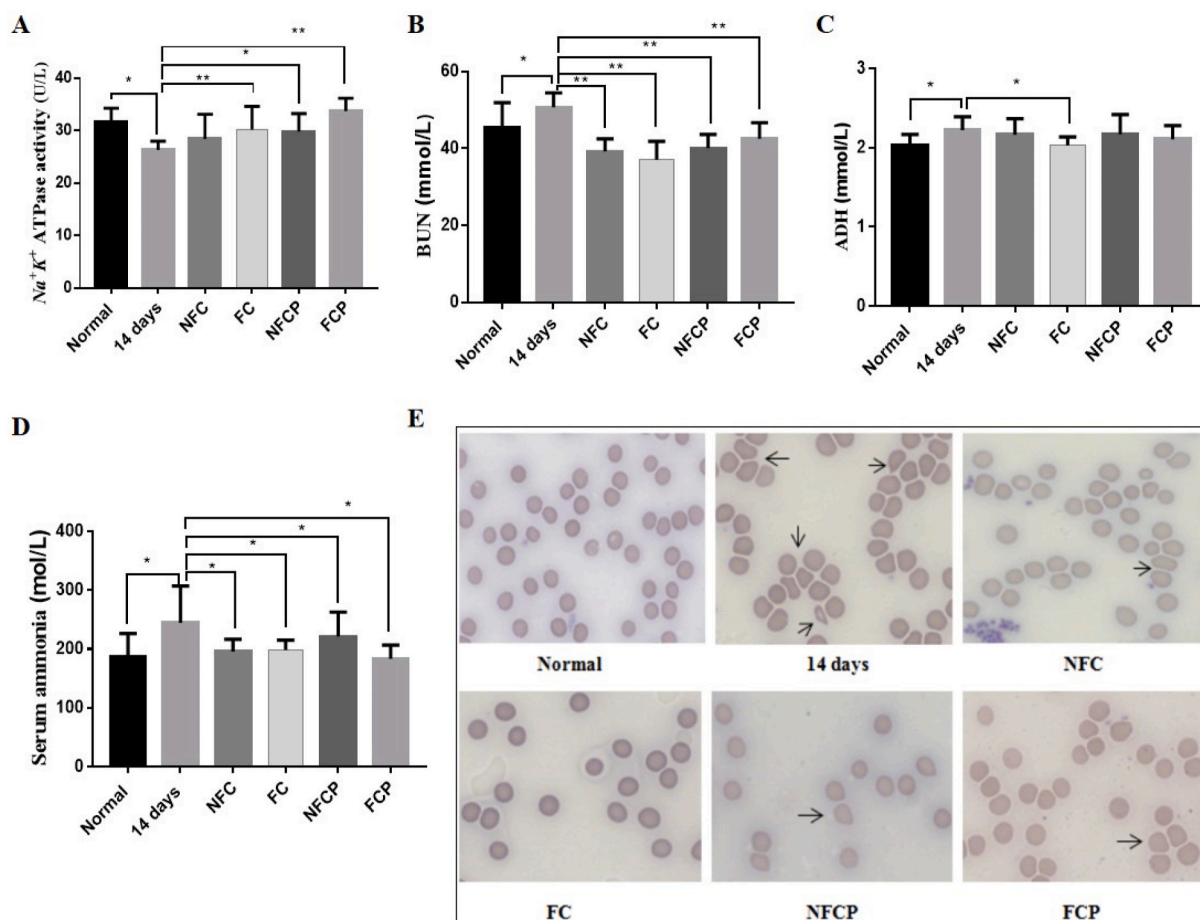


**Fig. 2.** The erythrocyte  $\text{Na}^+/\text{K}^+$  ATPase activity (A), ADH (B), BUN (C), ammonia (D) and Giemsa stained peripheral blood smears (E) of mice. The arrows indicate abnormal erythrocyte morphology. Representative images were taken with  $63 \times$  magnifications.

supernatant was concentrated and precipitated by 70% (v/v) alcohol. The fermented coix seed polysaccharides (FCP) and non-fermented coix seed polysaccharides (NFPC) was obtained by dialyzing and lyophilizing.

#### 2.4. Analytical methods

Molecular weights (Mw) and homogeneity of NFPC and FCP were detected by the high performance gel permeation chromatography, monosaccharide composition analysis was referred to the methods of the previous report (Shi et al., 2017). Neutral sugar content was determined according to the phenol- $\text{H}_2\text{SO}_4$  method with mannose as standard. Content of total uronic acid was determined by the m-hydroxydiphenyl assay, using glucuronic acid as standard. Protein content was determined by spectrophotometric method using bovine serum albumin (0.00, 0.02, 0.04, 0.06, 0.08, 0.10 mg/mL) as the standard.

#### 2.5. Experimental animals and design

Male BALB/c mice (8 weeks old,  $20 \pm 2$  g) were purchased from Vital River Laboratories (VRL, Beijing, China). The mice were acclimated for 1 week under the control conditions of temperature ( $23 \pm 2$  °C) and humidity ( $50 \pm 5\%$ ) in a 12/12 day/night cycle environment and fed on the same batch of standard laboratory diet (VRL, Beijing, China). All animals used in this study were cared for in accordance with the Guidelines for the Care and Use of Laboratory Animals published by the United States National Institute of Health (NIH, Publication No. 85-23, 1996), and all procedures were approved by the Animal Care Review

Committee (Animal application approval number 0064257), Nanchang University, China.

After the adaptation, all the mice were randomly divided into six groups ( $n = 10$ ), as shown in Fig. 1 A. Mice kept in the animal room under normal temperature ( $23 \pm 2$  °C) and humidity ( $50 \pm 5\%$ ) for 14 days were classified the normal group. Mice were kept in the man-made climate box (RXZ-500C-5, Ningbo jiangnan instrument factory, China) under normal temperature ( $23 \pm 2$  °C) and high RH ( $90 \pm 2\%$ ) for 14 days were classified the 14 days group. Mice exposed to high RH environment were given 14-day oral administration of 0.1 mL FC/NFC or 200 mg/(kg-bw) NFPC/FCP were classified the FC, NFC, NFPC and FCP groups, respectively. The Normal and 14 days groups were orally given water at about 9:00 a.m. every day. After fasting 12 h, all mice were weighed and then sacrificed by cervical dislocation after taking peripheral blood samples from the orbit, half in centrifuge tube with dipotassium EDTA and half in centrifuge tube without dipotassium EDTA. Feces samples were collected at the 6th, 8th, 11th, 12th, 13th and 14th day, and stored at  $-80$  °C for further analyses.

#### 2.6. Erythrocyte $\text{Na}^+/\text{K}^+$ ATPase activity, plasma ADH and BUN levels, serum ammonia examination

The blood samples in centrifuge tube with dipotassium EDTA and without dipotassium EDTA were firstly allowed to come to room temperature for 1 h, and then centrifuged at 827 g for 20 min to separate the plasma and serum supernatant, respectively. A transparent and uniform hemolytic solution was prepared according to previous study (Yin et al., 2022), then erythrocyte  $\text{Na}^+/\text{K}^+$  ATPase activity of the hemolytic

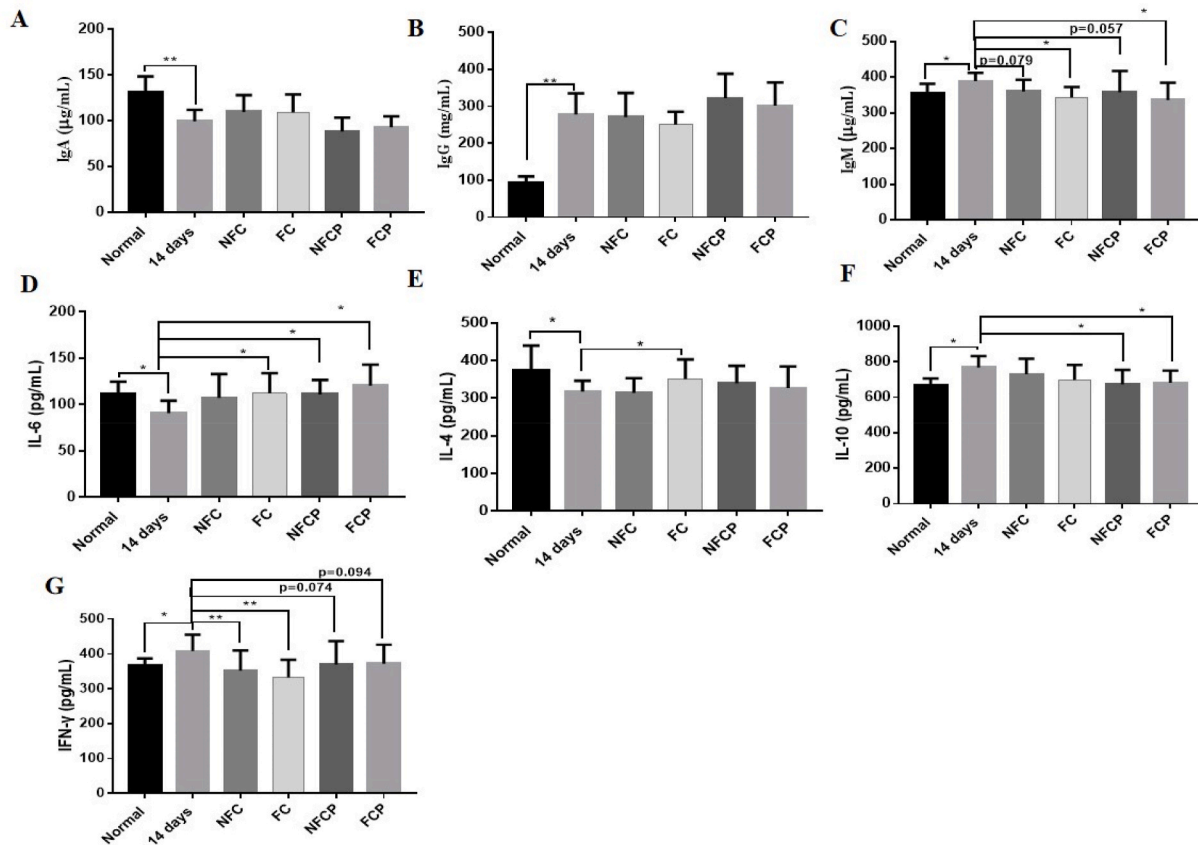


Fig. 3. Plasma levels of IgA (A), IgG (B), IgM (C) and cytokines IL-6 (D), IL-4 (E), IL-10 (F), IFN- $\gamma$  (G) of mice.

solutions was analyzed by ELISA kit. The plasma ADH, BUN and serum ammonia contents were measured using commercially available kits.

## 2.7. Quantification of plasma immune globulin and cytokines levels

The blood samples in centrifuge tube with dipotassium EDTA were allowed to come to room temperature for 1 h, and then centrifuged at 827 g for 20 min to separate the plasma supernatant. The plasma globulin IgA, IgM, IgG and cytokines IL-6, IL-4, IL-10, IFN- $\gamma$  contents were analyzed by ELISA kits according to the method provided by commercially available kits.

## 2.8. Fecal moisture, pH and short-chain fatty acids detection

The fecal moisture was measured using a rapid moisture tester (Sartorius MA100, Sartorius, Germany). The fecal pH values were determined using a pH meter (LAQUAtwin pH-33, HORIBA, Ltd., Japan). The SCFAs contents were detected following the gas chromatography method (Hu et al., 2012).

## 2.9. Gut microbiota analysis

Feces DNA samples were prepared using a TIANamp stool DNA Kit (Tiangen biotech Beijing co., LTD, China). The extracted DNA samples were checked for quality and concentration by 1% agarose gel electrophoresis and ultraviolet spectroscopy (Nanodrop ND-1000, Thermo Electron Corporation, USA). The V4 hypervariable regions of the bacterial 16S rRNA gene were amplified by PCR using primers 515F (5'-barcode-GTGCCAGCMGCGCGTAA-3') and 806R (5'-GGAC-TACHVGGGTWTCTAAT-barcode-3') (García-García et al., 2019). Final PCR products were purified to remove unincorporated nucleotides and primers using the Qiaquick PCR Purification kit (Qiagen, Germany).

Purified amplicons were quantified by using Agilent 2100 Bioanalyzer (Agilent Technologies, USA) with the High Sensitivity DNA Kit (Chips Reagents) (Agilent Technologies, USA), and were subjected to paired-end sequencing ( $2 \times 250$  bp) on an Illumina Miseq platform (Illumina Inc., San Diego, CA, USA) according to standard protocols. Quality filtering was performed using fastq with default settings. For downstream analysis, the retained reads with an average length of 225 bp were processed with the open-source bioinformatics pipeline Quantitative Insights into Microbial Ecology (QIIME) (Caporaso et al., 2010). Chimeric sequences were removed by the Usearch method and the sequences were grouped into operational taxonomic units (OTUs) by UCLUST with a minimum of 97% sequence similarity. From each OTU, representative sequences (most abundant) were aligned using the Python nearest Alignment Space Termination (PyNAST), and taxonomy was assigned by the Greengenes database (v.13\_8). For alpha diversity, the OTU table was rarefied at an even sampling depth of 7050 sequences/sample.

## 2.10. Statistical analysis

All results were subjected to statistical analysis by one-way ANOVA with the Least Significant Difference (LSD) test using SPSS 19.0 (SPSS Inc., Chicago, IL, USA). Difference in  $\beta$ -diversity was performed in R 3.6.0 by using bray-curtis metrics and packages of "vegan" and "ggplot2". Data with  $*p < 0.05$  and  $**p < 0.01$  were considered statistically significant and extremely significant, respectively, while  $0.1 \geq p \geq 0.05$  were considered as tendency. All data are shown as mean  $\pm$  standard deviation (SD).

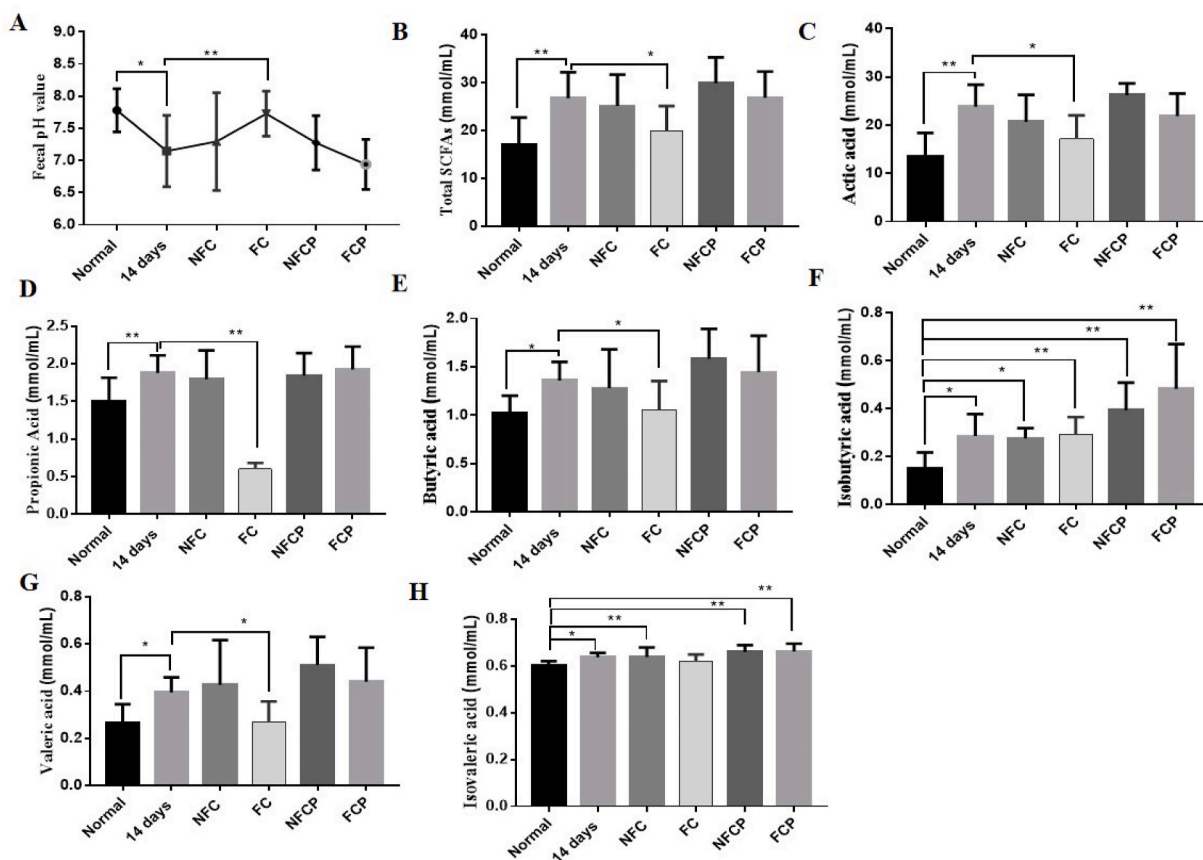


Fig. 4. Fecal pH values (A), total SCFAs levels (B) and changes of SCFAs profile (C–H) of mice.

### 3. Results and discussion

#### 3.1. Chemical characterization of NFECF and FCP

The extraction yields of NFECF and FCP were  $179.80 \pm 8.00\%$  and  $359.27 \pm 79.75\%$ , respectively (Table 1). This data was in agreement with our previous report in which the content of soluble dietary fiber was increased significantly in coix seed after fermented with *L. plantarum* NCU137 (Yin et al., 2020). The uronic acid and protein contents were dropped after fermentation from 10.42% to 9.05% and 4.07%–1.37% (w/w), respectively. No apparent difference was observed in neutral sugar contents and monosaccharide compositions between NFECF and FCP (Table 1). Our data indicated that NFECF and FCP were glucans, containing about 10% protein. These data was consistent to the report that water-soluble polysaccharides from coix seeds was resolved into 7 glucans, and 2 of them contained 8–11% protein (Yamada et al., 1985). The Mw of polysaccharides were less after fermentation (Fig. 1 B), which was in agreement with that *L. plantarum* NCU116 fermentation lowered the Mw of polysaccharides from *Momordica charantia* L. (Gao et al., 2018). It might contributed to *Lactobacillus plantarum* could utilize carbohydrate substrates by the carbohydrate-active enzyme (CAZY) (Mao et al., 2021). These results indicated that fermentation could decrease the Mw and alter chemical composition of coix seed polysaccharides.

#### 3.2. NFC, FC and polysaccharides improved the appearance of feces by increasing fecal moisture

After high RH exposure, the appearance of feces in the 14 days group was inconsistent which was dry and rough or wet, when compared with the normal group. However, the fecal appearance was consistent and moist after treatments, especially in the FC group (Fig. 1 D)). When we

monitored the fecal water content, we found that the fecal moisture was significantly decreased from  $51.27 \pm 1.51\%$  to  $30.44 \pm 0.28\%$  ( $p < 0.01$ ) after 6-day high RH exposure, whereas significantly increased ( $p < 0.01$ ) after 13-day exposure in the 14 days group relative to the normal group. However, the fecal water contents in all intervention groups were significantly increased throughout the experimental period ( $p < 0.01$ ) (Fig. 1). It might be contributed to the strong water-holding capacity for colonic content of plant polysaccharides (Hu et al., 2012; Teferra, 2021; Zhang et al., 2021). These results indicated an improved fecal appearance via increasing fecal moisture in response to NFC, FC and polysaccharides supplementation.

#### 3.3. FC, FCP and NFECF improved erythrocyte morphology and decreased circulating nitrogen in mice

Compared with the normal group, the erythrocyte  $\text{Na}^+/\text{K}^+$  ATPase activity was markedly decreased ( $p < 0.01$ ) in the 14 days group (Fig. 2 A). Meanwhile, plasma ADH was increased from  $2.03 \pm 0.13$  mmol/L to  $2.22 \pm 0.17$  mmol/L ( $p < 0.05$ , Fig. 2 C) after 14-day exposure, and accompanied by a rise in plasma BUN and serum ammonia ( $p < 0.05$ , Fig. 2 B, D). The above indices were all recovered significantly with the treatment of FC. Except for ADH, other indices were improved significantly in the FCP and NFECF groups. However, only plasma BUN ( $p < 0.01$ ) and serum ammonia ( $p < 0.05$ ) contents were lowered in the NFC group. ADH was suggested to be the major physiological regulator of renal water excretion and blood volume (Gassanov et al., 2011). However, our results suggested that the lowering of plasma BUN level might be relevant to the ADH level and erythrocyte  $\text{Na}^+/\text{K}^+$  ATPase activity. Data from recent experiments suggested that urea is toxic that induces molecular changes related to insulin resistance, free radical production, apoptosis and disruption of the protective intestinal barrier (Vanholder et al., 2018). As a source of ammonia, urea is converted to ammonia by

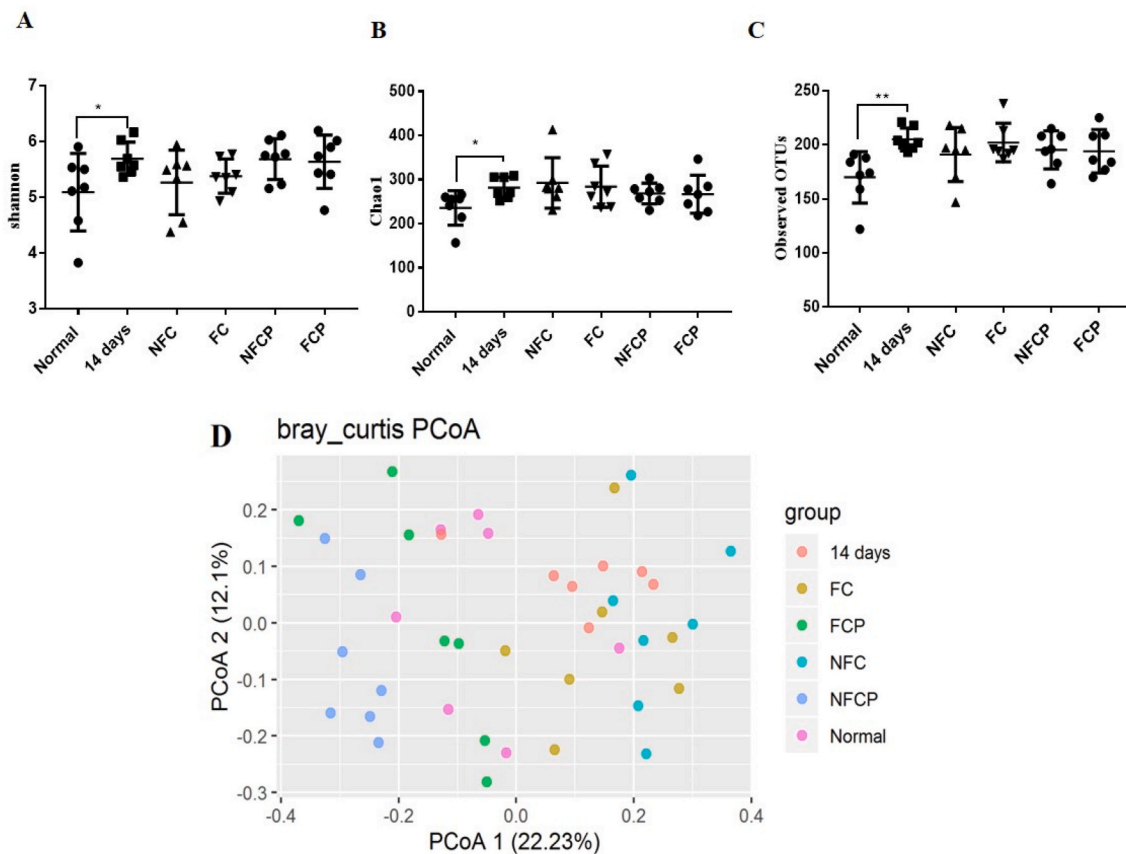


Fig. 5.  $\alpha$ -phylogenetic diversity Shannon (A), Chao1(B) and observed OTUs (C) and Principal co-ordinates analysis at the bray\_curtis operational taxonomic units (OTU) level (D). M  $\pm$  SD, n = 7.

urease expressed by intestinal bacteria (Vaziri, 2016; Yin et al., 2022). The increasing blood ammonia is an important causative factor in hepatic encephalopathy, which clinical treatment is focused on lowering ammonia (David and Michael, 2018). Circulating urea and ammonia were reduced after the intervention with NFC, FC and polysaccharides.

Based on the remarkable variation in  $\text{Na}^+/\text{K}^+$  ATPase activity, we tested erythrocyte morphology by Giemsa staining. Following the evaluation standard of peripheral blood smear (Jones, 2009), the erythrocyte morphology in the normal group was smooth, round-shaped, and uniform size. Compared to the normal group, the erythrocyte showed a bigger and deformed shape, which made these bizarre red cells distinct from other cells in the 14 days group. With the treatment of FC, NFPC and FCP, the red blood cells were almost restored to normal morphology via promoting erythrocyte  $\text{Na}^+/\text{K}^+$  ATPase activity (Fig. 2 E).

### 3.4. FC and FCP restored immune homeostasis by regulating Th1/Th2 cytokines and immunoglobulin

Researchers have long found that high ambient humidity can influence human immune profiles (Gao et al., 2019). Here, we found that plasma immunoglobulin IgA decreased significantly ( $p < 0.01$ ), while IgG and IgM increased significantly ( $p < 0.01$ ) in the 14 days group compared to the normal group (Fig. 3 A, B and C). Moreover, plasma cytokines IL-6 (from  $111.46 \pm 13.24$  to  $90.87 \pm 13.37$  pg/mL,  $p < 0.05$ ) and IL-4 (from  $374.35 \pm 65.42$  to  $318.31 \pm 28.25$  pg/mL,  $p < 0.05$ ) were reduced significantly, while IL-10 (from  $666.59 \pm 39.36$  to  $796.05 \pm 64.48$  pg/mL,  $p < 0.05$ ) and IFN- $\gamma$  (from  $366.16 \pm 21.25$  to  $408.32 \pm 46.42$  pg/mL,  $p < 0.05$ ) increased significantly (Fig. 3D–G). IFN- $\gamma$  is regarded as a marker for Th1 responses, while IL-4 is a markers for Th2 responses, and IL-10 is classified as both Th1 and Th2 cytokine

(Francisca, 2007). After high RH exposure, Th1 cytokine IFN- $\gamma$  increased while Th2 cytokine IL-4 reduced. Therefore, these data indicated that high RH exposure induced Th1/Th2 cytokine imbalance that resulted in immune dysfunction.

In traditional Chinese medicine, coix seed exerts stimulating the function of spleen (Zhu, 2017). In recently years, researchers claimed that coix seed had various immunomodulatory activities (Suzuki and Konaya, 2021). In comparison, with treatments of FC and FCP, the level of IgM decreased significantly ( $p < 0.01$ ), IgM ( $p < 0.01$ ) and IFN- $\gamma$  levels were down-regulated, anti-inflammatory cytokine IL-6 level was up-regulated. Meanwhile, plasma IL-10 ( $p < 0.05$ ) decreased significantly with the treatment of polysaccharides (Fig. 3 D, E, F and G). Taken together, these data suggested that FC and FCP could more effectively regulate immune function of mice exposing to high RH by regulating Th1/Th2 cytokines and immunoglobulin.

### 3.5. FC and polysaccharides regulated the production of SCFAs in mice exposing to high RH

Compared to the normal group, the fecal pH value went down sharply ( $p < 0.05$ ), and the total SCFAs level increased correspondingly in the 14 days group, which might be relative to increased colonic urea nitrogen metabolism due to more urea flux entry. Particularly, the level of acetic acid ( $p < 0.01$ ), butyric acid ( $p < 0.05$ ), valeric acid ( $p < 0.05$ ) and propionic acid ( $p < 0.05$ ), as well as branched-chain fatty acids (BCFAs), e.g. isobutyric acid ( $p < 0.05$ ) and isovaleric acid ( $p < 0.01$ ) rose significantly (Fig. 4). Gut-derived microbial metabolites SCFAs, play an important role in host health (Sridharan et al., 2014). However, some studies indicated that overproduction or accumulation of SCFAs in the bowel, such as acetate may lead to obesity, due to the increased energy accumulation (Perry et al., 2016), propionic acid is positively

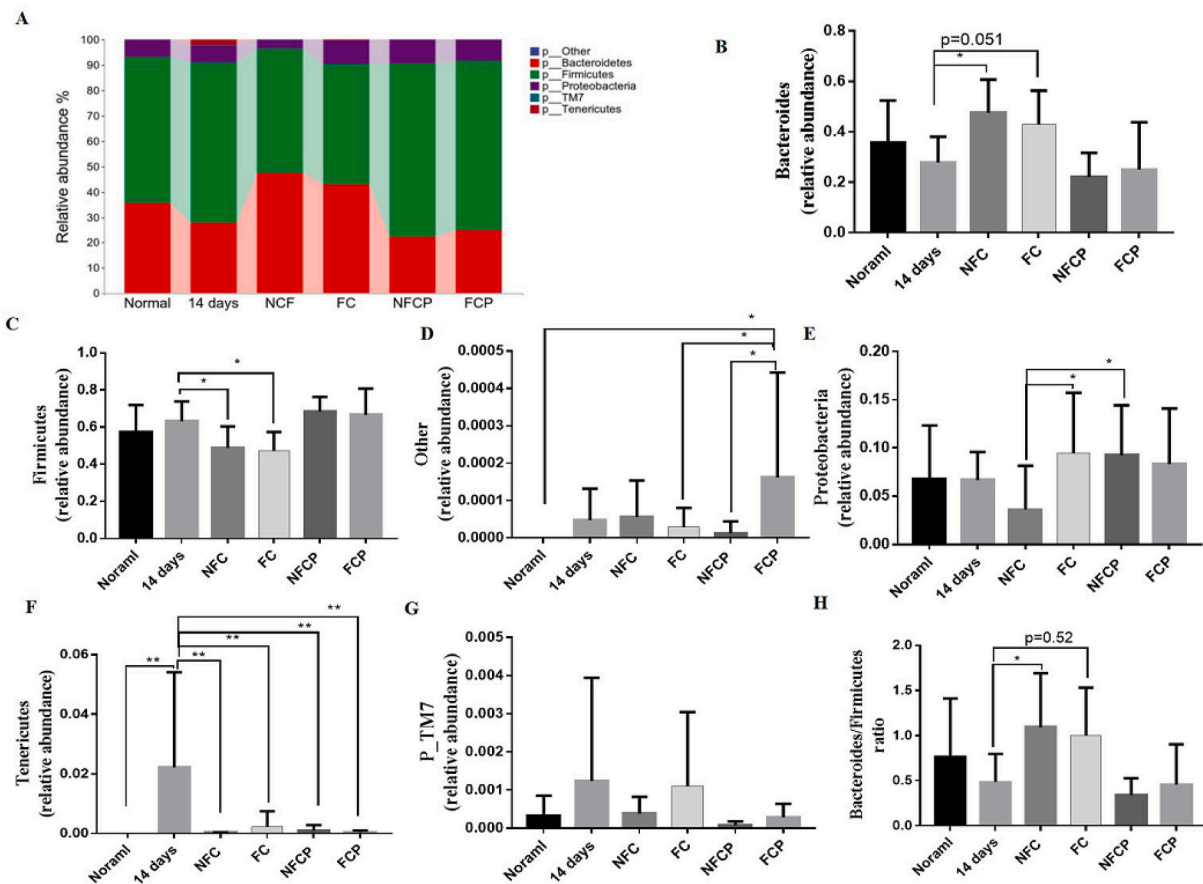


Fig. 6. Fecal microbiota composition at phylum level (A) and differences of bacterial relative abundance among groups (B–F). M ± SD, n = 7.

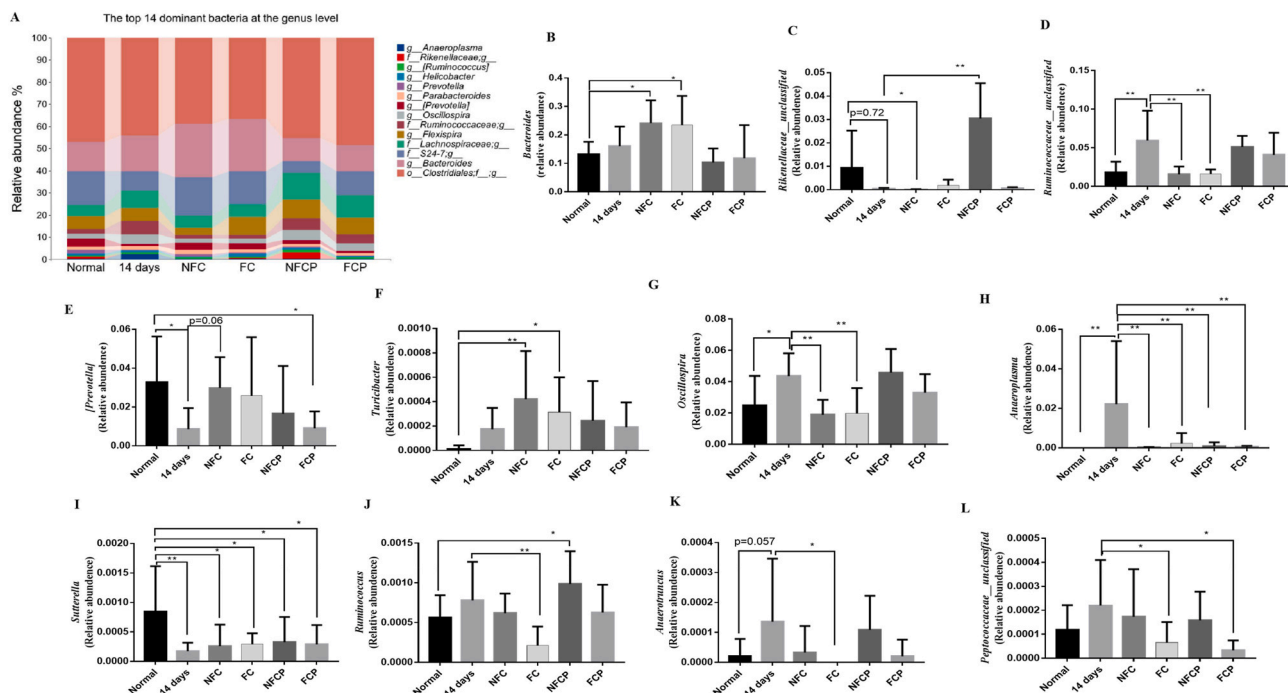
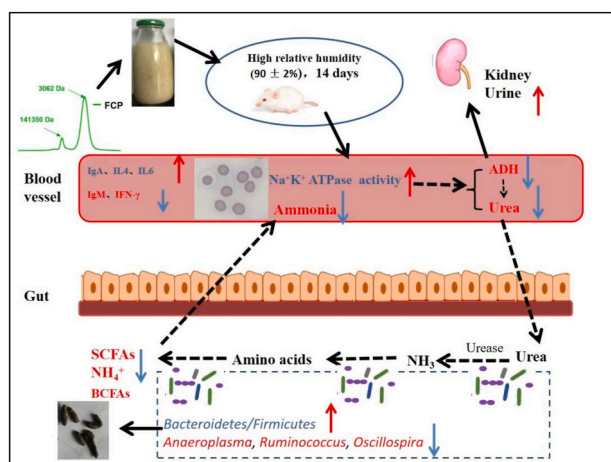


Fig. 7. The top 16 dominant bacteria at the genus level (A) and differences of bacterial relative abundance among groups (B–L). M ± SD, n = 7. *[Prevotella]* is Bacteroidales\_Paraprevotellaceae\_Prevotella.



**Fig. 8.** Schematic representation for effects of fermented coix seed and polysaccharides on circulating nitrogen, immune function and gut microbiota in mice exposed to high relative humidity.

correlated with development of diabetes mellitus (Sanna et al., 2019), and butyrate overproduction seems to be a risk factor for the development of metabolic disease (Chen et al., 2019; Stoeva et al., 2021). With the supplementation of FC, the fecal pH value increased significantly ( $p < 0.01$ ) with the SCFAs level reducing. These results suggested that FC could regulate SCFAs contents significantly in mice exposing to high RH.

Polysaccharides are favorable to proliferate SCFAs-producing bacteria to improve intestinal microenvironment by promoting SCFAs production (Tang et al., 2019). With the supplementation of polysaccharides, the levels of fecal SCFAs increased significantly ( $p < 0.05$ ), corresponding with the pH value decreased significantly ( $p < 0.01$ ) when compared to the normal group (Fig. 4 A, B). SCFAs including acetate, butyrate and propionate are the key bacterial metabolites that can contribute to develop and maintain the immune system (Koh et al., 2016), which might explain that FCP effectively regulated immune function of mice exposing to high RH by SCFAs (Fig. 3). On the other hand, SCFAs provided gut microbiota with energy for growth and nitrogen incorporation, in turn, increasing fecal bacteria mass and nitrogen excretion (Younes et al., 2006). Taken together, FCP and NFPCP might increase nitrogen excretion through fecal excretion, and regulate immune function in mice exposing to high RH via increasing the production of intestinal SCFAs.

### 3.6. FC and FCP reshaped gut microbiota in mice

Compared with the normal group, the  $\alpha$ -diversity indices of Shannon ( $p < 0.05$ ), Chao1 ( $p < 0.05$ ) and observed OTUs ( $p < 0.01$ ) increased significantly in the 14 days group (Fig. 5). The result was consistent with literature reported that Chao1 and Shannon indices increased significantly in gut microbiota of mice exposing to high temperature ( $30 \pm 0.5$  °C) and high humidity (85–90%) for 8 consecutive weeks (Chen et al., 2019). With the treatments of NFC, FC, NFPCP and FCP, no significant change was found among the  $\alpha$ -diversity.

The  $\beta$ -diversity analysis based on bray-curtis metrics showed that the 5 exposure groups could be distinguished from the normal group, while the 4 treatment groups were different from the 14 days group (Fig. 5 D). Adonis test confirmed that the  $\beta$ -diversity of the 14 days group ( $p = 0.0003$ ) was significant different from the normal group, and the  $\beta$ -diversity of the NFC ( $p = 0.006$ ), FC ( $p = 0.026$ ), NFPCP ( $p = 0.0003$ ) and FCP ( $p = 0.0030$ ) groups were significantly different from the 14 days groups.

At phylum level, the relative abundance of Tenericutes was significant higher in the 14 days group ( $p < 0.05$ ) when compared to the normal group, but reduced after all the treatment (Fig. 6 F). With the

supplementation of NFC or FC, the relative abundance of Bacteroidetes increased ( $p < 0.05$ ), while the relative abundance of Firmicutes reduced ( $p < 0.05$ ). These resulted in a higher Bacteroidetes-to-Firmicutes ratio in the NFC ( $p < 0.05$ ) and FC ( $p = 0.052$ ) groups (Fig. 6 B, C, H), which was negatively correlated with the yield of SCFAs (Antje et al., 2015).

Changes at genus level were shown in Fig. 7. After 14-day high RH exposure, the relative abundances of *Bacteroidales\_Paraprevotellaceae\_Prevotella* ( $p < 0.05$ ), *Rikenellaceae\_unclassified* ( $p < 0.05$ ), *Sutterella* ( $p < 0.01$ ), *Anaerostipes* ( $p < 0.05$ ) and *Prevotella* ( $p = 0.097$ ) were lower than the normal group, while the abundances of *Ruminococcaceae\_unclassified* ( $p < 0.01$ ), *Lachnospiraceae\_unclassified* ( $p < 0.05$ ), *Oscillospira* ( $p < 0.05$ ), *Anaeroplasmata* ( $p < 0.05$ ) and *Anaerotruncus* ( $p = 0.057$ ) were enriched. In all the treatment groups, the relative abundances of *Anaeroplasmata* ( $p < 0.01$ ) involving in the biosynthesis of one or more aromatic amino acids (Petzel and Hartman, 1990) were significantly lower than that in the 14 days group (Fig. 7 H). Moreover, with the supplementation of NFC or FC, the relative abundances of *Oscillospira* ( $p < 0.01$ ) were reduced, which was a butyrate producing bacteria (Gophna et al., 2017). However, the relative abundances of *Peptococcaceae\_unclassified* ( $p < 0.05$ ), an amino acid-fermenting bacteria that can utilize glutamine, leucine, phenylalanine and serine to produce SCFAs (Dai et al., 2011), was lower in FC and FCP groups. *Ruminococcus*, a acetic acid and formic acid producing bacteria (Domingo et al., 2008) also reduced significantly in the FC group. These results showed that NFC, FC and polysaccharides could reshape gut microbiota composition to varying degrees in mice exposing to high RH. It implied that FC and FCP could decrease the relative abundance of gut microbe involved in the biosynthesis of aromatic amino acids and SCFAs.

## 4. Conclusion

Taken together, the yield of FCP was richer after *L. plantarum* NCU137 fermentation, with the Mw reduced and chemical composition altered. In the intervention experiment, FCP and FC could not only restore the morphology of erythrocyte by promoting  $\text{Na}^+/\text{K}^+$  ATPase activity in high RH exposure mice, but also improve the circulating nitrogen by reducing the plasma BUN, serum ammonia, which might relate with the reducing abundance of microbe involved in the biosynthesis of amino acids and SCFAs. Furthermore, the immune function was also modulated by regulating Th1/Th2 cytokines and immunoglobulin production (Fig. 8). Our results indicated that FCP might be the efficacy composition in FC. Further study should focus on the purification, structure and efficacy on circulating nitrogen and immune function of FCP, as well as determination whether gut microbiota is the main target in this model by fecal bacteria transplantation. Our research provides new insights into developing coix seed-based effective and safe intervening strategies for the prevention of immune function and circulating nitrogen disordered.

## Compliance and ethics

The authors have declared no conflict of interest.

## CRediT authorship contribution statement

**Hui Wang:** Conceptualization, Investigation, Methodology, Formal analysis, Writing – original draft. **Hongmei Yin:** Conceptualization, Investigation, Formal analysis, Writing – review & editing, Funding acquisition. **Yadong Zhong:** Conceptualization, Investigation, Writing – review & editing. **Jielun Hu:** Writing – review & editing, Funding acquisition. **Shengkun Xia:** Investigation. **Zixuan Wang:** Investigation. **Shaoping Nie:** Supervision. **Mingyong Xie:** Supervision, Conceptualization, Funding acquisition.



## Declaration of competing interest

The authors declare that they have no known competing financial interests or personal relationships that could have appeared to influence the work reported in this paper.

## Acknowledgments

Key Program of National Natural Science Foundation of China (32130082), Jiangxi high level talent cultivation project (20204BCJ24006), Key Technology Project in Jiangxi Province (20212AAF01005), Central Government Guide Local Special Fund Project for Scientific and Technological Development of Jiangxi Province (20212ZDD02008) and Open Project Program of State Key Laboratory of Food Science and Technology, Nanchang University (No. SKLF-KF-202219) were gratefully acknowledged.

## Abbreviations used

IFN- $\gamma$	interferon- $\gamma$ ;
IL-6	interleukin-6
IL-10	interleukin-10
IL-4	interleukin-4
IgA	immunoglobulin A; I
gM	immunoglobulin M
IgG	immunoglobulin G
RH	relative humidity
ADH	antidiuretic hormone
BUN	blood urea nitrogen
SCFAs	short-chain fatty acids

## References

- Antje, D.M., Suparna, M., Schollenberger, A.E., Michael, K.K., Tobias, M., Alfred, K.N., Huson, D.H., Bischoff, S.C., 2015. Effects of surgical and dietary weight loss therapy for obesity on gut microbiota composition and nutrient absorption. *BioMed Res. Int.* 806248, 2015.
- Caporaso, J.G., Kuczynski, J., Stombaugh, J., Bittinger, K., Bushman, F.D., Costello, E.K., Fierer, N., Peña, A.G., Goodrich, J.K., Gordon, J.I., Huttley, G.A., Kelley, S.T., Knights, D., Koenig, J.E., Ley, R.E., Lozupone, C.A., McDonald, D., Muegge, B.D., Pirrung, M., Reeder, J., Sevinsky, J.R., Turnbaugh, P.J., Walters, W.A., Widmann, J., Yatsunenko, T., Zaneveld, J., Knight, R., 2010. QIIME allows analysis of high-throughput community sequencing data. *Nat. Methods* 7 (5), 335–336.
- Chen, P.C., Chien, Y.W., Yang, S.C., 2019. The alteration of gut microbiota in newly diagnosed type 2 diabetic patients. *Nutrition* 63–64, 51–56.
- Chen, S., Zheng, Y., Zhou, Y., Guo, W., Tang, Q., Rong, G., Hu, W., Tang, J., Luo, H., 2019. Gut dysbiosis with minimal enteritis induced by high temperature and humidity. *Sci. Rep.* 9 (1), 1–10.
- Chen, M., Xiao, D., Liu, W., Song, Y., Zou, B., Li, L., Li, P., Cai, Y., Liu, D., Liao, Q., Xie, Z., 2020. Intake of *Ganoderma lucidum* polysaccharides reverses the disturbed gut microbiota and metabolism in type 2 diabetic rats. *Int. J. Biol. Macromol.* 155, 890–902.
- Dai, Z.L., Wu, G., Zhu, W.Y., 2011. Amino acid metabolism in intestinal bacteria: links between gut ecology and host health. *Front. Biosci.* 16 (1), 1768–1786.
- David, L., Michael, L., 2018. A model of blood-ammonia homeostasis based on a quantitative analysis of nitrogen metabolism in the multiple organs involved in the production, catabolism, and excretion of ammonia in humans. *Clin. Exp. Gastroenterol.* 11, 193–215.
- Davila, A.M., Blachier, F., Gotteland, M., Andriamihaja, M., Benetti, P.H., Sanz, Y., Tomé, D., 2013. Re-print of “Intestinal luminal nitrogen metabolism: role of the gut microbiota and consequences for the host”. *Pharmacol. Res.* 69 (1), 114–126.
- De Filippis, F., Pasoli, E., Ercolini, D., 2020. The food-gut axis: lactic acid bacteria and their link to food, the gut microbiome and human health. *FEMS Microbiol. Rev.* 44 (4), 454–489.
- Domingo, M.C., Huletsky, A., Boissinot, M., Bernard, K.A., Picard, F.J., Bergeron, M.G., 2008. *Ruminococcus gauvreauii* sp. nov., a glycopeptide-resistant species isolated from a human faecal specimen. *Int. J. Syst. Evol. Microbiol.* 58 (6), 1393–1397.
- Fang, Y.K., Huang, B.S., Zhang, Y., Liu, H.F., Zou, C.Y., 2021. Polysaccharide derived from pomelo seed coat ameliorates APAP-induced liver injury in hybrid grouper (*Epinephelus lanceolatus*  $\times$  *Epinephelus fuscoguttatus*). *eFood* 2 (6), 319–325.
- Flint, H.J., Bayer, E.A., Rincon, M.T., Lamed, R., White, B.A., 2008. Polysaccharide utilization by gut bacteria: potential for new insights from genomic analysis. *Nat. Rev. Microbiol.* 6 (2), 121–131.
- Francisca, M., 2007. Cytokine responses to *Schistosoma haematobium* in a Zimbabwean population: contrasting profiles for IFN- $\gamma$ , IL-4, IL-5 and IL-10 with age. *BMC Infect. Dis.* 7 (1), 139.
- Gao, H., Wen, J.J., Hu, J.L., Nie, Q.X., Chen, H.H., Xiong, T., Nie, S.P., Xie, M.Y., 2018. Polysaccharide from fermented *Momordica charantia* L. with *Lactobacillus plantarum* NCU116 ameliorates type 2 diabetes in rats. *Carbohydr. Polym.* 201, 624–633.
- Gao, X., Colicino, E., Shen, J., Kioumourtzoglou, M.A., Just, A.C., Nwanaji-Enwerem, J. C., Coull, B., Lin, X., Vokonas, P., Zheng, Y., Hou, L., Schwartz, J., Baccarelli, A.A., 2019. Impacts of air pollution, temperature, and relative humidity on leukocyte distribution: an epigenetic perspective. *Environ. Int.* 126, 395–405.
- García-García, N., Tamames, J., Linz, A.M., Pedrós-Alió, C., Puente-Sánchez, F., 2019. Microdiversity ensures the maintenance of functional microbial communities under changing environmental conditions. *ISME J.* 13 (12).
- Gassanov, N., Semmo, N., Semmo, M., Nia, A.M., Fuhr, U., Er, F., 2011. Arginine vasopressin (AVP) and treatment with arginine vasopressin receptor antagonists (vaptans) in congestive heart failure, liver cirrhosis and syndrome of inappropriate antidiuretic hormone secretion (SIADH). *Eur. J. Clin. Pharmacol.* 67 (4), 333–346.
- Gophna, U., Konikoff, T., Nielsen, H.B., 2017. *Oscillospira* and related bacteria – from metagenomic species to metabolic features. *Environ. Microbiol.* 19.
- Hu, J.L., Nie, S.P., Min, F.F., Xie, M.Y., 2012. Polysaccharide from seeds of *Plantago asiatica* L. Increases short-chain fatty acid production and fecal moisture along with lowering pH in mouse colon. *J. Agric. Food Chem.* 60 (46), 11525–11532.
- Jian, X., Zhu, Y., Ouyang, J., Wang, Y., Lei, Q., Xia, J., Guan, Y., Zhang, J., Guo, J., He, Y., Wang, J., Li, J., Lin, J., Su, M., Li, G., Wu, M., Qiu, L., Xiang, J., Xie, L., Jia, W., Zhou, W., 2020. Alterations of gut microbiome accelerate multiple myeloma progression by increasing the relative abundances of nitrogen-recycling bacteria. *Microbiome* 8 (1), 74.
- Jones, K.W., 2009. Evaluation of cell morphology and introduction to platelet and white blood cell morphology. *Clin. Hematol. Fund. Hemost.* 93–116.
- Koh, A., De Vadder, F., Kovatcheva-Datchary, P., Bäckhed, F., 2016. From dietary fiber to host physiology: short-chain fatty acids as key bacterial metabolites. *Cell* 165 (6), 1332–1345.
- Kurmi, K., Haigis, M.C., 2020. Nitrogen metabolism in cancer and immunity. *Trends Cell Biol.* 30 (5), 408–424.
- Lavelle, A., Sokol, H., 2020. Gut microbiota-derived metabolites as key actors in inflammatory bowel disease. *Nat. Rev. Gastroenterol. Hepatol.* 17 (4), 223–237.
- Lin, H., Zhang, J., Li, S., Zheng, B., Hu, J., 2021. Polysaccharides isolated from *Laminaria japonica* attenuates gestational diabetes mellitus by regulating the gut microbiota in mice. *Food Frontiers* 2, 208–217.
- Ling, C.W., Miao, Z., Xiao, M.L., Zhou, H.w., Jiang, Z., Fu, Y., Xiong, F., Liu, Y.p., Wu, Y. y., Jing, L.p., 2020. The association between gut microbiota and osteoporosis was mediated by amino acid metabolism: multi-omics integration in a large adult cohort. *J. Clin. Endocrinol. Metabol.* <https://doi.org/10.1101/2020.08.28.20183764>.
- Mao, B., Yin, R., Li, X., Cui, S., Zhang, H., Zhao, J., Chen, W., 2021. Comparative genomic analysis of *Lactiplantibacillus plantarum* isolated from different niches. *Genes* 12 (2).
- Ni, J., Shen, T.C.D., Chen, E.Z., Bittinger, K., Bailey, A., Roggiani, M., Sirota-Madi, A., Friedman, E.S., Chau, L., Lin, A., 2017. A role for bacterial urease in gut dysbiosis and Crohn's disease. *Sci. Transl. Med.* 9 (416), eaah6888.
- Perry, R.J., Peng, L., Barry, N.A., Cline, G.W., Zhang, D., Cardone, R.L., Petersen, K.F., Kibbey, R.G., Goodman, A.L., Shulman, G.I., 2016. Acetate mediates a microbiome–brain– $\beta$ -cell axis to promote metabolic syndrome. *Nature* 534 (7606), 213–217.
- Petzel, J.P., Hartman, P.A., 1990. Aromatic amino acid biosynthesis and carbohydrate catabolism in strictly anaerobic mollicutes (*Anaeroplasmata* spp.). *Syst. Appl. Microbiol.* 13 (3), 240–247.
- Sanna, S., van Zuydam, N.R., Mahajan, A., Kurilshikov, A., Vich Vila, A., Vösa, U., Mujagic, Z., Masclee, A.A.M., Jonkers, D.M.A.E., Oosting, M., Joosten, L.A.B., Netea, M.G., Franke, L., Zhernakova, A., Fu, J., Wijmenga, C., McCarthy, M.I., 2019. Causal relationships among the gut microbiome, short-chain fatty acids and metabolic diseases. *Nat. Genet.* 51 (4), 600–605.
- Shi, X.D., Nie, S.P., Yin, J.Y., Que, Z.Q., Zhang, L.J., Huang, X.J., 2017. Polysaccharide from leaf skin of *Aloe barbadensis* Miller: Part I. Extraction, fractionation, physicochemical properties and structural characterization. *Food Hydrocolloids* 73, 176–183.
- Song, Q., Wang, Y., Huang, L., Shen, M., Yu, Y., Yu, Q., Chen, Y., Xie, J., 2021. Review of the relationships among polysaccharides, gut microbiota, and human health. *Food Res. Int.* 140, 109858.
- Sridharan, G.V., Choi, K., Klemashevich, C., Wu, C., Prabakaran, D., Pan, L.B., Steinmeyer, S., Mueller, C., Yousofshahi, M., Alaniz, R.C., Lee, K., Jayaraman, A., 2014. Prediction and quantification of bioactive microbiota metabolites in the mouse gut. *Nat. Commun.* 5 (1), 5492.
- Stoeva, M.K., Garcia-So, J., Justice, N., Myers, J., Tyagi, S., Nemchek, M., McMurdie, P. J., Kolterman, O., Eid, J., 2021. Butyrate-producing human gut symbiont, *Clostridium butyricum*, and its role in health and disease. *Gut Microb.* 13 (1), 1907272.
- Suzuki, Y., Konaya, Y., 2021. Coix seed may affect human immune function. *Nat. Prod. Commun.* 16 (10), 1934578X211048642.
- Tang, C., Ding, R., Sun, J., Liu, J., Kan, J., Jin, C., 2019. The impacts of natural polysaccharides on intestinal microbiota and immune responses—a review. *Food Funct.* 10 (5), 2290–2312.
- Teferra, T.F., 2021. Possible actions of inulin as prebiotic polysaccharide: a review. *Food Frontiers* 2, 407–416.
- Vanholder, R., Gryp, T., Glorieux, G., 2018. Urea and chronic kidney disease: the comeback of the century?(in uraemia research). *Nephrol. Dial. Transplant.* 33 (1), 4–12.
- Vaziri, N.D., 2016. Effect of synbiotic therapy on gut-derived uremic toxins and the intestinal microbiome in patients with CKD. *Am Soc Nephrol* 11, 199–201.

- Yamada, H., Yanahira, S., Kiyohara, H., Cyong, J.C., Otsuka, Y., 1985. Water-soluble glucans from the seed of *Coix lacryma-jobi* var. *ma-yuen*. *Phytochemistry* 25 (1), 129–132.
- Yang, W., Ren, D., Zhao, Y., Liu, L., Yang, X., 2021. Fuzhuan brick tea polysaccharide improved ulcerative colitis in association with gut microbiota-derived tryptophan metabolism. *J. Agric. Food Chem.* 69 (30), 8448–8459.
- Yin, H.M., Wang, S.N., Nie, S.P., Xie, M.Y., 2018. Coix polysaccharides: gut microbiota regulation and immunomodulatory. *Bioact. Carbohydr. Diet. Fibre.* 16, 53–61.
- Yin, H.M., Zhong, Y.D., Xia, S.K., Hu, J.L., Nie, S.P., Xiong, T., Xie, M.Y., 2020. Effects of fermentation with *Lactobacillus plantarum* NCU137 on nutritional, sensory and stability properties of Coix (*Coix lacryma-jobi* L.) seed. *Food Chem.* 314, 126037.
- Yin, H.M., Zhong, Y.D., Wang, H., Hu, J.L., Xia, S.K., Xiao, Y.D., Nie, S.P., Xie, M.Y., 2022. Short-term exposure to high relative humidity increases blood urea and influences colonic urea-nitrogen metabolism by altering the gut microbiota. *J. Adv. Res.* 35, 153–168.
- Younes, H., Egret, N., Hadj-Abdelkader, M., Rémésy, C., Demigné, C., Gueret, C., Deteix, P., Alphonse, J.C., 2006. Fermentable carbohydrate supplementation alters nitrogen excretion in chronic renal failure. *J. Ren. Nutr.* 16 (1), 67–74.
- Yu, Q., Chen, W., Zhong, J., Huang, D., Shi, W., Chen, H., Yan, C., 2022. Purification, structural characterization, and bioactivities of a polysaccharide from *Coreopsis tinctoria*. *Food Frontiers*. <https://doi.org/10.1002/fft2.145>.
- Zhang, Y.J., Xie, Q.T., You, L.J., Cheung, P.C., Zhao, Z.G., 2021. Behavior of non-digestible polysaccharides in gastrointestinal tract: a mechanistic review of its anti-obesity effect. *eFood* 2 (2), 59–72.
- Zhu, F., 2017. Coix: chemical composition and health effects. *Trends Food Sci. Technol.* 61, 160–175.